

# Nanostructure of Au–20%Pd layers in MoS<sub>2</sub> multilayer solid lubricant films

G. Jayaram<sup>a</sup>, L.D. Marks<sup>a</sup>, M.R. Hilton<sup>b,\*</sup>

<sup>a</sup> Department of Materials Science and Engineering, Northwestern University, Evanston, IL 60208, USA

<sup>b</sup> Mechanics and Materials Technology Center, The Aerospace Corporation, El Segundo, CA 90245, USA

## Abstract

High-resolution electron microscopy imaging and electron and X-ray diffraction techniques have been used to characterize the structure of low and high flux Au–20%Pd layers in Au–20%Pd/MoS<sub>2</sub> multilayer solid lubricant thin films. Images clearly reveal different morphologies for the metal layers in the two flux regimes, which can be correlated to the variation in fracture resistance reported by an earlier indentation study. In the lower metal flux regime, three-dimensional islands with single-crystal and multiply twinned structures are seen, while quasi-continuous, polycrystalline regions are seen in the higher flux case.

*Keywords:* Solid lubricants; Multilayer films; Transmission electron microscopy; Fracture toughness

## 1. Introduction

Sputter-deposited MoS<sub>2</sub> films incorporating periodic metal multilayers of Au–20%Pd (henceforth referred to as Au–Pd) or Ni were first developed for use as solid lubricants in high-cycle mechanisms on spacecraft [1]. Such films generally have dense microstructures, with significant basal plane orientation ((001) parallel to the substrate), as determined by X-ray diffraction (XRD) [2]; the presence of multilayers appears to suppress and/or interrupt the competitive nucleation and growth of edge-plane facets that would lead to the evolution of porous columnar plate (zone 2) morphologies [2].

Studies of the tribological performance of Au–Pd multilayer films in sliding contact and in rolling element bearings indicated that these films had better endurance than the zone 2 films [2,3]. However, spallation of both zone 2 and some multilayer films from the surface to the substrate were reported to occur early in rolling contact tests [4–6]. While spalled material can transfer onto unlubricated components (e.g. bearing balls and/or retainer pockets), and facilitate particle lubrication in certain applications, such as those using thrust bearings, it is deleterious in others, such as torque-sensitive angular contact bearings [3]; for the latter case, control of film fracture toughness is required.

Multilayer film fracture toughness, as measured by

brale indentation [2,6], was seen to depend on metal layer periodicity and nominal metal layer thickness. For Ni–MoS<sub>2</sub> multilayer films, fracture around the indentation was inhibited by decreasing the metal layer periodicity, i.e. for a constant film total thickness, increasing the number of multilayers. Increasing metal layer thickness, particularly above a critical value, also improved fracture resistance. Based on these early indentation studies, Hopple et al. [7] investigated the fracture/spallation resistance of Au–Pd/MoS<sub>2</sub> films as a function of metal layer thickness under indentation and rolling contact. At 10 nm periodicity, films with 5 nm thick metal layers had better fracture resistance than films with 1.5 nm metal layer thickness when the total thickness was held at 400 nm. The 5 nm Au–Pd/10 nm films (where the values before and after “/” represent the thickness and periodicity of the metal layers respectively) also performed better than 1.5 nm Au–Pd/10 nm films in endurance and torque tests involving angular contact bearings. These studies suggested that the respective microstructures were responsible for the variation in the behaviour of these films.

Structural characterization of multilayer Au–Pd/MoS<sub>2</sub> films to date has been carried out using XRD and scanning electron microscopy (SEM) [2]. The data from these techniques are consistent with a simple model that assumes alternating continuous layers of metal and MoS<sub>2</sub>. In all these studies, the stated thicknesses of the metal layers are estimated, i.e. not measured, and are

\* Corresponding author.

extrapolations from the deposition rates of thicker films, with the layers assumed to be continuous and of uniform thickness. The validity of these assumptions is assessed in this paper, which reports the first investigation to characterize, using high-resolution transmission electron microscopy (HREM), transmission electron diffraction (TED) and XRD, the nanostructure of the Au–Pd layers in MoS<sub>2</sub> multilayer films.

## 2. Experimental procedures

Au–Pd/MoS<sub>2</sub> multilayer films were prepared by r.f. magnetron sputtering with argon at 0.266 Pa pressure and at room temperature (for further details see Ref. [2]). Plan-view TEM samples were prepared by sequentially depositing Au–Pd and MoS<sub>2</sub> layers onto carbon films. The following (nominal) compositions were prepared:

- (a) 1.5 nm Au–Pd + 8.5 nm MoS<sub>2</sub>: single and double bilayers
- (b) 5.0 nm Au–Pd + 5.0 nm MoS<sub>2</sub>: single and double bilayers

An Au–Pd/MoS<sub>2</sub> sequence constitutes a single bilayer, and a repeat of this unit is a double bilayer. In order to attain a better general understanding of the structural transformations between the single and double bilayers for the low and high Au–Pd compositions, trilayers (i.e. Au–Pd/MoS<sub>2</sub>/Au–Pd) of the corresponding compositions were also studied. Individual metal films of the two thicknesses, pure MoS<sub>2</sub> films and reverse bilayer films (Au on MoS<sub>2</sub>) were also prepared to obtain characterization data that was used to interpret the structural data of the bilayer films.

HREM and TED data were collected from the above films using a 300 kV Hitachi H9000 microscope. For XRD studies, 1.5 nm Au–Pd/10 nm and 5 nm Au–Pd/10 nm films with total thicknesses of 1  $\mu$ m were prepared on 440C steel substrates. The above thickness values are extrapolated from deposition parameters established for thicker films and, for reasons that are detailed in the discussion section, we shall refer to these films as low flux ( $\leq 1.5$  nm Au–Pd) or high flux films ( $\geq 5$  nm Au–Pd) in the remainder of the paper.

## 3. Results

### 3.1. HREM and TED

Prior to characterizing the structural differences, if any, between the bilayers at the two different flux regimes, HREM images and TED patterns were recorded from the constituent pure Au–Pd films deposited on carbon substrates. These data revealed gross

differences in the microstructure in the two cases. Discrete three-dimensional (3D) metal islands were seen in the low flux films, suggesting a Volmer–Weber type growth mode. These 3D islands had a mixture of single crystals and multiply twinned structures, as shown in Fig. 1 (this mixed morphology growth is similar to that seen in the cases of Au and Ag deposited on carbon and silicon monoxide substrates [8,9]) and ranged in size between 2.5 and 5 nm. The islands' sizes explain the diffuse rings seen in the TED pattern inset of Fig. 1. In the high flux films, the metal layers were seen to have a quasi-continuous, polycrystalline nature, as shown in Fig. 2, suggestive of coalescence at later stages of growth; the polycrystalline domain sizes range between 5 and 10 nm. The inset TED pattern shows polycrystalline rings with spacings that could all be indexed using pure Au as a reference. The quasi-continuous nature of the film became apparent when tilting the film brought off-axis Au–Pd nanometre-size grains into lattice imaging conditions.

MoS<sub>2</sub> deposited onto both low and high flux metal films, thus forming a single bilayer, had a very dense microstructure with extremely small domains of basal islands (i.e. it has short-range order) coexisting with some edge islands. This interpretation was confirmed by looking at MoS<sub>2</sub> films deposited directly onto carbon substrates where the same coexisting microstructure of small basal island domains and edge islands was observed.

TED patterns recorded from the double bilayer films showed differences from the corresponding single bilayer cases: the (002) ring of MoS<sub>2</sub> was faintly visible in both cases, while an extremely weak (100) ring of MoS<sub>2</sub> was also seen in the 5 nm Au–Pd case. (A generic increase in intensities, and sharpening, specifically in the low flux case, of the Au–Pd rings was also observed.) This corresponded to the presence of hexagonal basal island domains of MoS<sub>2</sub> in high flux films, as shown in Fig. 3; however, no such domains were seen in the low flux films. In order to understand better the reasons behind the differing microstructure of MoS<sub>2</sub> in the two flux regimes, and the intensity of the Au–Pd rings in the TED patterns, trilayer and reverse bilayer films were also studied. An explanation for the intensity increase of the Au–Pd rings was obtained by contrasting the microstructure of the trilayer films with the single bilayer ones.

TED patterns in both compositional cases in such trilayer films showed an increase in the intensity of the Au–Pd rings from the corresponding single bilayer cases, which would be consistent with an increase in the metal content. Images revealed that, in addition, an increase in the domain size of the 3D islands was the cause for the ring sharpening in the low flux films. Such domain size increases can be explained by virtue of the fact that, since in the low flux films Au–Pd forms discrete 3D



Fig. 1. The typical microstructure of a low flux Au–Pd film deposited on a carbon substrate: three-dimensional (3D) islands comprising of single crystals and multiply twinned particles; “T” arrows show twins in the latter. The inset diffraction pattern of the region in the image shows diffuse rings corresponding to the small sizes of these particles; the (111) ring of Au–Pd is arrowed for reference.

islands on carbon substrates, MoS<sub>2</sub> deposited on such single layers can be expected to grow primarily on the exposed carbon substrate. Deposition of Au–Pd on these films would therefore lead to coalescence with the existing 3D Au–Pd islands, resulting in larger domains. On the other hand, in the high flux case, MoS<sub>2</sub> growth would be on a quasi-continuous, polycrystalline Au–Pd underlayer, and further Au–Pd deposition on such bilayers would only lead to an increase in the Au–Pd content (by formation of a new quasi-continuous metal layer above the MoS<sub>2</sub> film).

The underlying assumption behind the above explanations is that the growth of Au–Pd on the MoS<sub>2</sub> surface of single bilayer films parallels that on carbon substrates. Therefore, reverse bilayers of the low and high flux compositions were also studied, and indeed, the growth mechanism was found to be identical to that on carbon i.e. 3D islands and quasi-continuous films of Au–Pd on MoS<sub>2</sub> respectively. Also, similar to observations from our earlier investigations of Au on MoS<sub>2</sub> under UHV conditions, Au–Pd growth was seen to occur on both the edge and basal island sites on the MoS<sub>2</sub> film [10].

### 3.2. XRD data

XRD scans of these multilayer films and pure MoS<sub>2</sub> and Au–Pd reference films are shown in Fig. 4. In the

pure MoS<sub>2</sub> films, the (002) reflection was the dominant one detected, corresponding to basal planes that are parallel to the substrate. (A small (100) reflection was also detected.)

The intensity of the detected (002) orientation dropped as the Au–Pd content increased, while reflections due to Au–Pd and from multilayers (labelled as ML) became clearly evident. We believe that this decrease in (002) intensity actually represents broadening of the XRD peak that occurs because the MoS<sub>2</sub> layers are very thin. In effect, the crystallite size of MoS<sub>2</sub> along the direction perpendicular to the film surface has become too small to generate a sharp diffraction peak, as predicted by the Scherrer equation [11]. This decrease in (002) intensity was also observed in Ni–MoS<sub>2</sub> films [2]. No (100) reflections were detected in the multilayer films.

## 4. Discussion

The combined data shows that nanostructures of multilayer metal–MoS<sub>2</sub> films are more complex than the simple model originally proposed [2] of alternating continuous layers of metal and basal-oriented MoS<sub>2</sub>. Au–Pd in the low flux regime, in these multilayer films, consists of islands that are not continuous. Higher

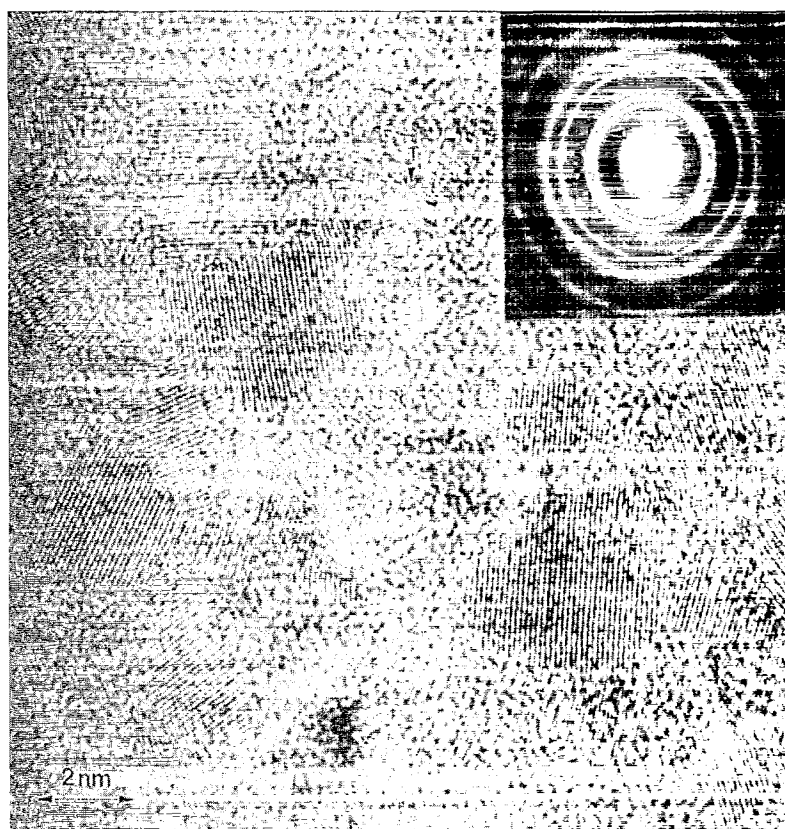


Fig. 2. The typical microstructure of a high flux Au-Pd film deposited on a carbon substrate: the quasi-continuous, polycrystalline nature of the film as opposed to discrete 3D islands in Fig. 1 is apparent; a twinned particle is arrowed and denoted by "T". The inset diffraction pattern shows sharp rings of polycrystalline Au-Pd domains; note also the stronger intensity of the Au-Pd(111) ring (arrowed).

concentrations appear to lead to coalescence of islands to form quasi-continuous layers. The terminology that has been used to describe the multilayer films, i.e. estimated metal layer thickness/periodic distance, is misleading. The ambiguity introduced by this procedure is the reason for the definition of films with estimated thicknesses of  $\leq 1.5$  nm as low flux films and those  $\geq 5$  nm as high flux films. We are assuming that the nanostructures of these single and double bilayer films are representative of films having more layers; cross-sectional and plan-view HREM studies of thicker films will be required to confirm this assumption.

A key finding of this investigation is that some edge island orientation is present in these films that is not detected by XRD of thicker multilayer films of the same composition. Thicker films grown at this pressure without metal layers can develop mixed orientations of basal and edge-oriented grains that are detected by XRD [2]; the grains have short-range order. The periodic interruption of MoS<sub>2</sub> deposition and incorporation of Au-Pd appear to be blocking the elongation of edge islands and repeatedly capturing a largely, but not exclusively, basal-oriented near-interface nanostructure of MoS<sub>2</sub>. Low fluxes of metal that form islands can induce this nanostructure, possibly because disordered monolayers

or submonolayers of Au-Pd may exist between the metal islands – the TEM data is not definitive on this hypothesis. The data also show that basal-oriented regions of MoS<sub>2</sub> grown on either carbon or Au-Pd can have very short-range order. The short-range order is consistent with TEM studies of similar films grown at these low pressures [12,13]. In addition, recent EXAFS data on the multilayer films clearly identify MoS<sub>2</sub> clusters at short-range, i.e. the material is not amorphous [14].

The difference in metal continuity between the low and high flux films provides some insight to the indentation and rolling contact data of Hopple et al. [7], which showed that the high flux films had better fracture/spallation resistance than the low flux ones. Multilayers in composites improve fracture toughness by one of two mechanisms: increased plasticity or decohesion of weak multilayer interfaces. In the multilayer films, there may also be some type of synergistic deformation process involving both the metal and sulphide that blunt cracks. The present TEM data do not favour any particular mechanism; however, the limited thickness of the Au-Pd layers makes it doubtful that plasticity is the toughening mechanism. Multilayer decohesion seems more plausible. In addition, a recent study of Cu-Si multilayers by Leung et al. [15] revealed that the decohesion mecha-



(a)



(b)

Fig. 3. Morphology of double bilayer films of (a) low flux and (b) high flux metal compositions: 3D metal particles (G) and edge islands of  $\text{MoS}_2$  (E) are seen in (a) while Au-Pd grains (G) hexagonal domains of the basal islands (B) and edge islands (E) of  $\text{MoS}_2$  are clearly seen in (b).

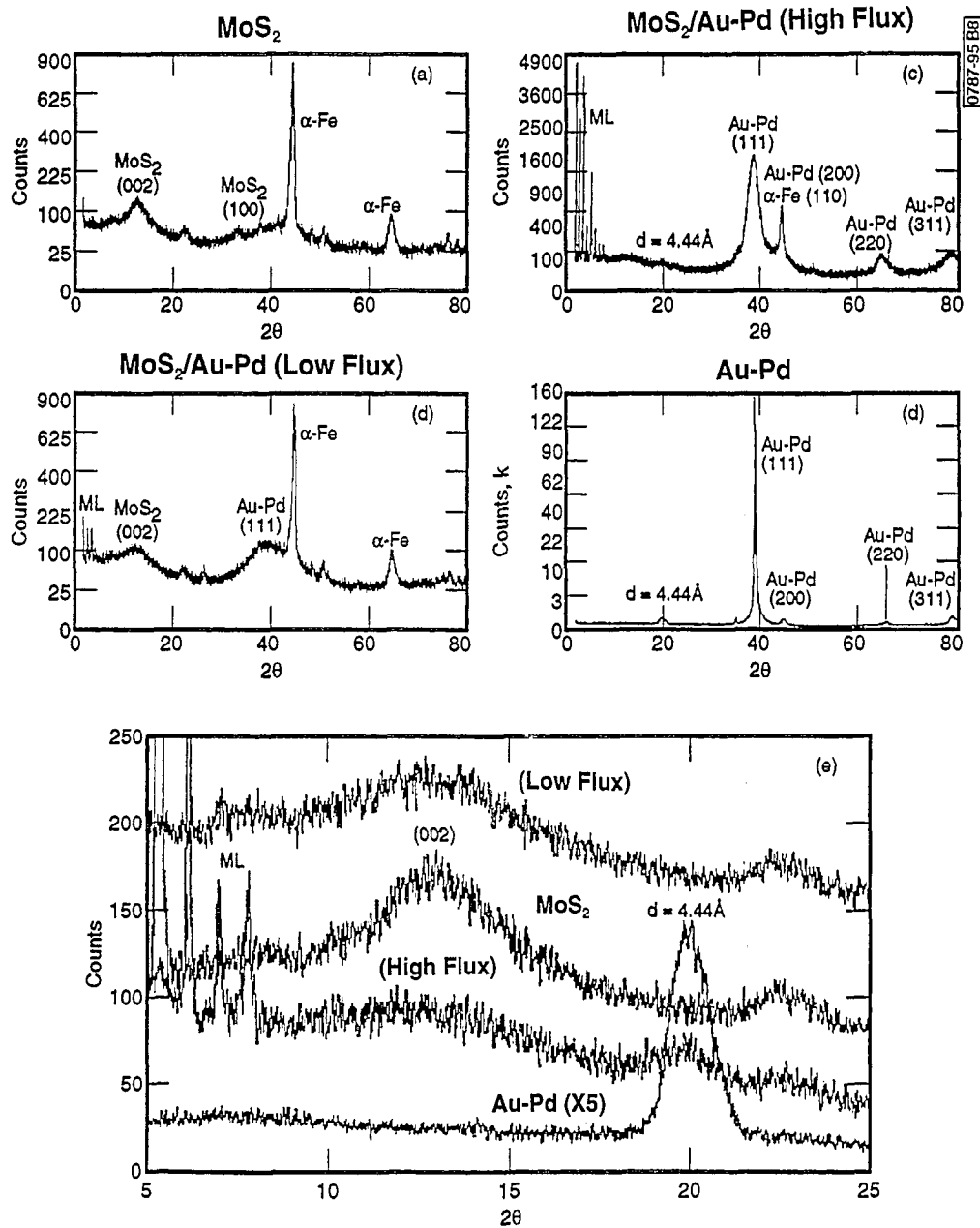


Fig. 4. XRD scans (log counts vs.  $2\theta$ ) of the pure  $\text{MoS}_2$  (a), low flux multilayer (b), high flux multilayer (c), and Au-20%Pd (d) reference films. The films are 1  $\mu\text{m}$  thick and were grown on steel. Major peaks due to the steel substrates are labelled, unlabelled minor peaks stem from steel or steel carbides. In the pure  $\text{MoS}_2$  films, the (002) basal orientation is detected and the intensity of the detected (002) orientation is seen to drop as Au-Pd content increases, as shown in (e), where absolute intensity is plotted in a linear scale – although the intensity of the Au-Pd reference film is scaled by a factor of 5. A weak (100)  $\text{MoS}_2$  reflection is detected in the pure non-multilayer film. Multilayer (ML) reflections also become evident. In both the pure Au-Pd and multilayer films, the (111) orientation of Au-Pd dominates. The peak of spacing  $d = 4.44 \text{ \AA}$  is associated with the presence of Au-20%Pd, but has not been uniquely identified.

nism was operative in films having periodicities of 50 to 500 nm. Multilayers do not directly enhance the fracture toughness of the film against lateral cracks running parallel to the film-substrate interface [16]. Instead, these multilayer toughening mechanisms can inhibit the propagation of radial cracks perpendicular to the film-substrate interface. Extensions of these radial cracks relieve tensile hoop stresses that would otherwise restrain lateral crack propagation. In the low flux films, we hypothesize that propagating cracks encounter particles,

which may blunt cracks more than pure  $\text{MoS}_2$  films. In the high flux films, it is probable that continuous metal layers generate more surface area or metal volume that blunt cracks more effectively.

Another benefit of such multilayer  $\text{MoS}_2$  might be improved oxidation resistance. The high degree of basal orientation of multilayer  $\text{MoS}_2$  is expected to provide these films with superior resistance to oxidation in humid storage [17]. Continuous layers of Au-Pd should improve oxidation resistance even further.

## 5. Conclusions

HREM and XRD studies have revealed that the nanostructure of Au–Pd/ MoS<sub>2</sub> films is more complex than previously assumed. The metal layers can consist of discrete islands, or be continuous with higher metal deposition promoting continuous layers. Previously estimated metal thicknesses based on deposition rates noted in earlier studies should be considered “flux thicknesses” for labelling or identification purposes, and not descriptions of the true layer thicknesses or structure. Both basal and edge-oriented MoS<sub>2</sub> domains are present in the MoS<sub>2</sub> layers, with the basal oriented MoS<sub>2</sub> having very short-range order. The continuity of the metal layers correlates well with improved fracture resistance observed in previous studies.

## Acknowledgements

This work was supported by the Aerospace Sponsored Research program and by the US Air Force Office of Scientific Research on Grant F49620-94-1-0164 AFOSR. The authors would like to thank Dr David Crowther (Wear Sciences/TA&T) for preparing the Au–Pd/MoS<sub>2</sub> multilayer films and Paul Adams (Aerospace) for obtaining the XRD data.

## References

- [1] M.R. Hilton and P.D. Fleischauer, *Surf. Coat. Technol.*, 54–55 (1992) 435.
- [2] M.R. Hilton, R. Bauer, S.V. Didziulis, M.T. Dugger, J. Keem and J. Scholhamer, *Surf. Coat. Technol.*, 53 (1992) 13.
- [3] S.H. Loewenthal, R.G. Chou, G.B. Hopple and W.L. Wenger, *Tribol. Trans.*, 37 (3) (1994) 505.
- [4] S.V. Didziulis, M.R. Hilton, R. Bauer and P.D. Fleischauer, Thrust bearing wear life and torque tests of sputter-deposited MoS<sub>2</sub> films, *Tech. Rep. TOR-92(2064)-1*, October 1992, The Aerospace Corporation.
- [5] G.B. Hopple and S.H. Loewenthal, *Surf. Coat. Technol.*, 68/69 (1994) 398.
- [6] M.R. Hilton, *Surf. Coat. Technol.*, 68/69 (1994) 407.
- [7] G.B. Hopple, J.E. Keem and S.H. Loewenthal, *Wear*, 162–164 (1993) 919.
- [8] S. Ino, *J. Phys. Soc. Jpn.*, 21 (1966) 346.
- [9] L.D. Marks and D.J. Smith, *J. Cryst. Growth*, 54 (1981) 425.
- [10] G. Jayaram, N. Doraiswamy, L.D. Marks and M.R. Hilton, *Surf. Coat. Technol.*, 68/69 (1994) 439.
- [11] B.D. Cullity, *Elements of X-ray Diffraction*, Addison-Wesley, Reading, MA, 1978, p. 102.
- [12] C. Muller, C. Menoud, M. Maillat and H.E. Hintermann, *Surf. Coat. Technol.*, 36 (1988) 351.
- [13] F. Levy and J. Moser, *Surf. Coat. Technol.*, 68/69 (1994) 433.
- [14] J.R. Lince, M.R. Hilton and A.S. Bommanavar, Metal Incorporation in sputter-deposited MoS<sub>2</sub> films studied by EXAFS, *J. Mater. Res.*, in press.
- [15] D.K. Leung, N.T. Zhang, R.M. McKeeking, and A.G. Evans, Crack progression and interface debonding in brittle/ductile nanoscale multilayers, *J. Mater. Res.*, in press.
- [16] A.G. Evans, Harvard University, personal communication, 5 August 1993.
- [17] P.D. Fleischauer, *ASLE Trans.*, 27 (1984) 82.